LUND UNIVERSITY

A Biophysical Model of Electrical Activity in Human β-Cells.

Pedersen, Morten Gram

Published in:
Biophysical Journal

DOI:
10.1016/j.bpj.2010.09.004

2010

Link to publication

Citation for published version (APA):
Pedersen, M. G. (2010). A Biophysical Model of Electrical Activity in Human β-Cells. *Biophysical Journal*, *99*(10), 3200-3207. https://doi.org/10.1016/j.bpj.2010.09.004

Total number of authors:
1

General rights
Unless other specific re-use rights are stated the following general rights apply:
Copyright and moral rights for the publications made accessible in the public portal are retained by the authors and/or other copyright owners and it is a condition of accessing publications that users recognise and abide by the legal requirements associated with these rights.
• Users may download and print one copy of any publication from the public portal for the purpose of private study or research.
• You may not further distribute the material or use it for any profit-making activity or commercial gain
• You may freely distribute the URL identifying the publication in the public portal

Read more about Creative commons licenses: https://creativecommons.org/licenses/

Take down policy
If you believe that this document breaches copyright please contact us providing details, and we will remove access to the work immediately and investigate your claim.

LUND UNIVERSITY

PO Box 117
221 00 Lund
+46 46-222 00 00

Download date: 18. Dec. 2025

LUND UNIVERSITY
Faculty of Medicine

LUP

Lund University Publications
Institutional Repository of Lund University

This is an author produced version of a paper published in Biophysical journal. This paper has been peer-reviewed but does not include the final publisher proof-corrections or journal pagination.

Citation for the published paper:

Morten Gram Pedersen

"A Biophysical Model of Electrical Activity in Human β-Cells."

Biophysical journal
2010, 99(10) pp. 3200 - 3207

http://dx.doi.org/10.1016/j.bpj.2010.09.004

Access to the published version may require journal subscription.

Published with permission from: Elsevier

A biophysical model of electrical activity in human β-cells

Morten Gram Pedersen[1],
Department of Information Engineering,
University of Padua, Italy
and
Lund University Diabetes Centre,
Department of Clinical Sciences,
Lund University, Sweden

[1]Current Address: Lund University Diabetes Centre, Department of Clinical Sciences, Clinical Research Centre, Lund University, CRC 91-11, UMAS entrance 72, SE-20502 Malmö, Sweden. E-mail: pedersen@dei.unipd.it, morten_gram.pedersen@med.lu.se

Abstract

Electrical activity in pancreatic β-cells plays a pivotal role in glucose-stimulated insulin secretion by coupling metabolism to calcium-triggered exocytosis. Mathematical models based on rodent data have helped in understanding the mechanisms underlying the electrophysiological patterns observed in laboratory animals. However, human β-cells differ in several aspects, and in particular in their electrophysiological characteristics, from rodent β-cells. Hence, from a clinical perspective and to obtain insight into the defects in insulin secretion relevant for diabetes mellitus, it is important to study human β-cells. This work presents the first mathematical model of electrical activity based entirely on published ion channel characteristics of human β-cells. The model reproduces satisfactorily a series of experimentally observed patterns in human β-cells, such as spiking and rapid bursting electrical activity, and their response to a range of ion channel antagonists. The possibility of human ether-a-go-go-related (HERG) and leak channels as drug targets for diabetes treatment is discussed based on model results.

Key words: Insulin; action potentials; ion channels; human islets, mathematical modeling.

Introduction

In response to raised blood glucose levels insulin is secreted from the pancreatic β-cells. Metabolism of the sugar leads to increased ATP/ADP ratio, closure of ATP-sensitive potassium channels (K(ATP)-channels) and electrical activity, which activates voltage-gated calcium channels. The resulting increase in intracellular calcium evokes insulin release through Ca^{2+}-dependent exocytosis. This pathway of insulin secretion is well-studied in rodents, and is also operating in humans (1–3).

The central role of electrical activity is highlighted by the excellent correlation between the fraction of time with electrical activity and insulin secretion (4). The plasma membrane potential in rodents shows complex bursting electrical activity with active phases where action potentials appear from a depolarized plateau, interspaced by silent, hyperpolarized phases (4–6). Mathematical modeling of electrical activity has for nearly 30 years accompanied the experimental investigations of the mechanisms underlying bursting electrical activity, starting with the ground-breaking work by Chay and Keizer (7) on which virtually all subsequent models, even the most recent, are based (8–11). β-cell models have been used to test, support and refute biological hypotheses (8, 10, 12), but frequently restricted to the most studied laboratory animals, in particular the mouse, due to the availability of electrophysiological data.

The interest in insulin secretion and pancreatic β-cells is caused by the central role of impaired insulin secretion in the development of the (human) disease diabetes mellitus. However, human β-cells show important differences to β-cells from mice, for example with respect to the patterns of electrical activity observed, which consist of very fast bursting or spiking in human cells (1, 3, 13–15), and never the classical slower burst pattern observed in rodents. This difference could be due to the involvement of different ion channels in human β-cells compared to rodents (1, 3, 14, 15) or to differences in islet organization (16, 17).

The present work presents the first biophysical model of electrical activity based on ion channel characteristics of human β-cells. Special attention has been given to choose model parameters directly from published, high-quality electrophysiological data, mainly from Braun et al. (3), who carefully assured that the investigated islet cells were indeed β-cells, but also from Rosati et al. (18), Herrington et al. (19) and Misler et al. (1). Using published parameters reduced parameter "tweaking" to a minimum. A similar approach was recently taken for modeling of murine β-cells (11). The presented model includes all voltage-gated currents found in human β-cells, and reproduces

a series of experimental data satisfactorily.

Methods

Modeling

Electrical activity is modeled by a Hodgkin-Huxley type model, as has been done for rodent β-cells (7–12, 20). Most voltage-gated membrane currents (measured in pA/pF) are modeled based on the results of Braun et al. (3), who carefully assured that investigated human islet cells were β-cells. Human ether-a-go-go-related (HERG) potassium currents in human β-cells were described by Rosati et al. (18) and are modeled accordingly.

The membrane potential V (measured in mV) develops in time (measured in ms) according to

$$\begin{aligned}\frac{dV}{dt} = -(&I_{HERG} + I_{BK} + I_{Kv} + I_{Na} \\ &+ I_{CaL} + I_{CaPQ} + I_{CaT} + I_{K(ATP)} + I_{leak}).\end{aligned} \tag{1}$$

In the following, the modeling of the currents on the right-hand side of Eq. 1 is explained in detail.

The leak current summarizes all currents not modeled explicitly, such as currents mediated by exchangers, pumps and, e.g., chloride and nonselective, non-voltage dependent cation channels, and is modeled as

$$I_{leak} = g_{leak}(V - V_{leak}). \tag{2}$$

The ATP-sensitive potassium current is described by

$$I_{K(ATP)} = g_{K(ATP)}(V - V_K). \tag{3}$$

Here, V_{leak} and V_K are the respective Nernst reversal potentials. Misler et al. (1) estimated that at 6 mM glucose, the conductances g_{leak} and $g_{K(ATP)}$ contribute to a similar extent to the total membrane conductance of ∼0.3 nS. With a cell capacitance of ∼10 pF (3), values of $g_{leak} = 0.015$ nS/pF and $g_{K(ATP)} = 0.015$ nS/pF are obtained for a glucose stimulated β-cell. These values are used as default, and can be found with all other default parameter values in Table 1.

Voltage-gated membrane currents are modeled as

$$I_X = g_X m_X h_X (V - V_{\tilde{X}}), \tag{4}$$

where X denotes the type of channels, $V_{\tilde{X}}$ the reversal potential of the ion $\tilde{X}$ conducted by the channels, while m_X describes activation and h_X describes inactivation of the channels. As described in the following, some channels are assumed not to inactivate (i.e., $h_X = 1$), some activate instantaneously ($m_X = m_{X,\infty}(V)$), but in general, activation (and similarly inactivation, h_X) is supposed to follow a first-order equation

$$\frac{dm_X}{dt} = \frac{m_{X,\infty}(V) - m_X}{\tau_{mX}}, \tag{5}$$

where τ_{mX} (respectively τ_{hX}) is the time-constant of activation (respectively inactivation for h_X), and $m_{X,\infty}(V)$ (respectively $h_{X,\infty}(V)$) is the steady-state voltage-dependent activation (respectively inactivation) of the current. The steady-state activation (and inactivation) functions are described with Boltzmann functions,

$$m_{X,\infty}(V) = \frac{1}{1 + \exp((V - V_{mX})/n_{mX})}, \tag{6}$$

except for calcium regulated currents as explained below. For activation functions, the slope parameter n_{mX} is negative, while the corresponding slope parameter n_{hX} is positive for inactivation functions.

As explained in the supplementary material, Ca^{2+} and Na^{+} reversal potentials were assumed different for the experiments used to characterize the currents, compared with the experiments measuring electrical activity (M. Braun, University of Oxford, UK, personal communications, 2010). The overall behavior of the model is not sensitive to this assumption, in particular spiking and bursting electrical activity can also be observed when V_{Ca} and V_{Na} are as in the experiments used to characterize the Ca^{2+} and Na^{+} currents. A detailed describtion of the currents of the model is given in the following.

Voltage-gated calcium channels

Braun et al. (3) found three types (T-, P/Q- and L-type) of voltage-gated Ca^{2+}-channels in human β-cells. The total Ca^{2+}-current activated very rapidly (<1 ms), and no difference in activation kinetics is apparent from the data using various Ca^{2+}-channel blockers (3, their Fig. 5). It is therefore assumed that all Ca^{2+}-channels activate instantaneously. The activation functions are estimated from the voltage-dependence of peak Ca^{2+}-currents reported by Braun et al. (3), and are given in Fig. S1 in the Supporting Material

The low-voltage activated T-type channels were found to inactivate faster than the L- and P/Q-types (3, their Fig. 5), and it is therefore assumed to be responsible for the fastest component of total Ca^{2+}-current inactivation with a time constant of $\tau_{hCaT} = 7$ ms. Braun et al. (3) found parameters of the Boltzmann function describing steady-state inactivation which are used here without modification.

The high-voltage activated P/Q-type channels are assumed not to inactivate, since they inactivate much more slowly than the other Ca^{2+}-currents and the duration of action potentials (3).

Finally, the high-voltage activated L-type Ca^{2+}-channels inactivate with a time-constant of $\tau_{hCaL} = 20$ ms (M. Braun, University of Oxford, UK, personal communications, 2010). The parameters of the inactivation function for L-type Ca^{2+}-channels in human beta-cells are unknown. However, the inactivation function of the total Ca^{2+}-current has been investigated (21). Inactivation showed a U-shaped voltage dependence with maximal inactivation of $\sim 50\%$ seen at -10 mV. Since L-type currents make up $\sim 50\%$ of total peak Ca^{2+}-currents in human β-cells (3), and T-type Ca^{2+}-channels are completely inactivated at -10 mV, while P/Q-type channels do not inactivate substantially (3), it was assumed that the U-shaped inactivation function reflects inactivation of the L-type Ca^{2+}-current with almost complete inactivation at -10mV. Inactivation of the L-type Ca^{2+}-current was assumed to be Ca^{2+}-dependent and caused mainly by Ca^{2+} in microdomains below the L-type channels (21, 22), which is approximately proportional to the L-type Ca^{2+} current (23). The amount of inactivation $(1 - h_{CaL,\infty})$ was therefore assumed proportional to the activated L-type Ca^{2+}-current $m_{CaL,\infty}(V)(V - V_{Ca})$, which yields the following expression for the inactivation function

$$h_{CaL,\infty}(V) = \max\left(0, \min\left\{1, 1 + [m_{CaL,\infty}(V)(V - V_{Ca})]/\Phi\right\}\right), \qquad (7)$$

with normalization factor $\Phi = 57$ mV (adjusted) and is shown in Fig. 1A. (The max-min construction confines h_{CaL} to the interval $[0, 1]$).

Voltage-gated sodium channels

Based on the rapid kinetics of the Na^{+}-currents (3), the voltage-gated sodium channels were assumed to activate instantaneously, and to inactivate with a time constant of 2 ms. The activation function is estimated from the voltage-dependence of peak Na^{+}-currents reported by Braun et al. (3), and are given in Fig. S2. Braun et al. (3) found parameters of the Boltzmann function describing steady-state inactivation which are used here without

modification. Both set of parameters are in good agreement with estimates by Barnett et al. (15).

Delayed rectifying potassium channels

The delayed rectifying potassium (Kv) channels were assumed to activate on a voltage-dependent time-scale (3, 19) as shown in Fig. 1B with expression

$$\tau_{mKv} = \begin{cases} \tau_{mKv,0} + 10 \exp\left(\frac{-20 \text{ mV} - V}{6\text{mV}}\right) \text{ ms}, & \text{for } V \geq 26.6 \text{ mV}, \\ \tau_{mKv,0} + 30 \text{ ms}, & \text{for } V < 26.6 \text{ mV}, \end{cases} \tag{8}$$

where (as default value) $\tau_{mKv,0} = 2$ ms (3). Note that Herrington et al. (19) found that Kv-channels activated more slowly with $\tau_{mKv,0} \approx 10$ ms. The Kv-current was assumed not to inactivate, because of its slow (seconds) inactivation kinetics (3, 19).

The activation function is estimated from the voltage-dependence of the Co^{2+}-resistant peak K^+-currents reported by Braun et al. (3), and are given in Fig. S3. The estimated values are in general agreement with (19, 21).

Large-conductance BK potassium channels

BK-channels show both voltage- and Ca^{2+}-dependence (24). However, since BK- and Ca^{2+}-channels are colocalized and BK-channel activation is regulated by local, microdomain Ca^{2+} below Ca^{2+}-channels (24), a simplification as done for L-type Ca^{2+}-channel inactivation can be done (23). The microdomain Ca^{2+}-concentration is assumed to be proportional to the total Ca^{2+}-current $I_{Ca} = I_{CaL} + I_{CaPQ} + I_{CaT}$. The steady-state activation function for BK-channels is therefore assumed to depend on V only, since it is assumed proportional to the product

$$[-I_{Ca}(V) + B_{BK}] \cdot m_{BK,\infty}(V)$$

where B_{BK} denotes 'basal', Ca^{2+}-independent, V-dependent activation, and $m_{BK,\infty}$ is a Boltzmann function as in Eq. 6. It is assumed that Ca^{2+}-dependent activation occurs instantaneously, while voltage-dependent activation follows Eq. 5 with time-constant $\tau_{mBK} = 2$ ms (3). BK-currents were assumed not to inactivate. This was done partly since the inactivation function of BK channels in human β-cells is unknown, and partly since BK-currents rapidly repolarize the membrane potential in most simulations, hence deactivation due to repolarization happens faster (~ 10 ms) than inactivation at depolarized membrane potentials (~ 22 ms, (3)).

The BK-current is then expressed as

$$I_{BK} = \bar{g}_{BK} m_{BK} (V - V_K)(-I_{Ca}(V) + B_{BK}), \tag{9}$$

with parameters chosen to reproduce the I-V relationship for the iberiotoxin (a specific BK-channel blocker) sensitive K^+-current reported by Braun et al. (3) and shown in Fig. S3B.

HERG potassium channels

The voltage-gated *human ether-a-go-go-related* (HERG) potassium channels are present in human β-cells (18, 25). Rosati et al. (18) found parameters of the Boltzmann activation and inactivation functions, which are used here without modification. The time-constant of inactivation was estimated from (18) to be ∼50 ms, while activation is slower. Based on data from ERG channels expressed in Xenopus oocytes (26), the activation time-constant is set to 100 ms. From results in Rosati et al. (18) a conductance of $g_{HERG} \sim 0.5$ nS/pF can be calculated. However, g_{HERG} increases with the extracellular K^+ concentration (27). Since Rosati et al. (18) used a relatively high extracellular K^+ concentration (40 mM) in their experiments, a lower value of $g_{HERG} = 0.2$ nS/pF was used in the model.

Numerical methods

Simulations were done in XPPAUT (28) by solving the differential equations using the cvode-solver with standard tolerances and time-step $dt = 0.02$ ms. The stochastic simulation in Fig. 5C, was done in XPPAUT with the backward Euler method with standard tolerances and $dt = 0.02$ ms (29). The computer code is available on `http://www.dei.unipd.it/~pedersen`.

Results

Spiking electrical activity

In response to glucose, human β-cells exhibit spiking electrical activity (1, 3, 18, 30). With the parameters estimated from results by Braun et al. (3) and Rosati et al. (18), and a K(ATP)-conductance of 0.015 nS/pF corresponding to 6 mM glucose (1), the model produces action potentials peaking at -8 mV with troughs at -68 mV (Fig. 2). The spike frequency is 4.6 Hz, which is slightly faster than experimental recordings (18, 31), but the frequency is sensitive to the assumed properties of the leak current I_{leak}. For example,

raising the leak Nernst potential V_{leak} increases the spike frequency, while lowering V_{leak} reduces the frequency (Fig. 2C). Similarly, raising the leak conductance, increases the spike frequency (Fig. 2B). This is because the membrane potential depolarizes faster, thus reducing the interspike interval. Glucose regulates electrical activity in human β-cells due to its metabolism, which results in increased ATP/ADP ratio and closure of K(ATP)-channels (1). With default parameters, the model produces spiking activity when the K(ATP) conductance $g_{K(ATP)}$ is less than ~ 0.019 nS/pF, while the membrane potential is silent and hyperpolarized for larger $g_{K(ATP)}$ values. The spike frequency is inversely related to the K(ATP) conductance (Fig. 2A). The value for $g_{K(ATP)}$ below which the model produces action potentials can be shifted by modulating the leak current. For example, raising the leak conductance two-fold to $g_{leak} = 0.030$ nS/pF increases the $g_{K(ATP)}$ threshold value to ~ 0.027 nS/pF.

Rosati et al. (18) showed that blocking HERG channels in human β-cells increased the glucose induced spike frequency by ∼30 %, in some cases by ∼50 %, suggesting an important role for HERG channels in controlling the timing of action potentials. Model simulations with standard parameters support this notion, since blocking the HERG current increases the spike frequency by 52 % from 4.6 Hz to 7 Hz (Fig. 2D). Moreover, the HERG channel activation time-constant plays a role in setting the spike frequency. For example, using $\tau_{m_{HERG}} = 500$ ms, a 5-fold increase but still in agreement with experiments (26), lowers the spike frequency to 4.0 (Fig. 2D). Blockage of HERG channels also shifts the $g_{K(ATP)}$ threshold value for electrical activities to ∼0.031 nS/pF.

Blocking voltage-dependent Na^+-channels in human β-cells with tetrodotoxin (TTX) reduces the action potential amplitude by 10-15 mV, and tends to broaden its duration (3, 15, 31). These results are captured by the model, though the reduction in peak voltage is slightly less (~ 5 mV) than observed experimentally (Figure 3Aa). With default parameters, setting $g_{Na} = 0$ nS/pF increases the interspike interval dramatically (by 44 % from 217 ms to 312 ms), but with lower K(ATP)-conductance the interspike interval is increased much less, e.g., by 9 % from 163 ms to 178 ms with $g_{K(ATP)} = 0.008$ nS/pF, and the main effect is on the action potential height (Figure 3B). The reduced spike frequency at high $g_{K(ATP)}$ values (reflecting low glucose concentrations), but not at low $g_{K(ATP)}$ values (raised glucose levels), might underlie the fact that TTX reduces insulin secretion less at high than at low glucose concentrations (3, 15). The model also reproduces (Fig. 3C) the facts that a T-type Ca^{2+}-channel antagonist reduces spike frequency and lowers action potential peak voltage slightly (3). Thus, the model simulations

support the ideas that the T-type Ca^{2+}-channels are involved in the timing of action potentials, and Na^{+}-currents shape the upstroke of the voltage spike (3, 15).

High-voltage activated L- and P/Q-type Ca^{2+}-currents are believed to be directly involved in exocytosis of secretory granules (1, 3, 32). Blocking L-type Ca^{2+}-channels suppresses electrical activity (3), which is reproduced by the model (Fig. 3C) and the lack of electrical activity is likely the main reason for the complete absence of glucose stimulated insulin secretion in the presence of L-type Ca^{2+}-blockers (3, 30).

Bursting electrical activity

The membrane potential of human β-cells often shows complex behavior (1, 13–15, 31) resembling bursting electrical activity in rodent β-cells located in islets (4–6), though the burst period (at most a few seconds) is much shorter in human β-cells. The model is able to reproduce such rapid bursting behavior by varying, for example, the assumed properties of the delayed rectifying potassium channels. Shifting the activation curve $m_{Kv,\infty}$ to the right (Fig. 4A), or reducing the total conductance g_{Kv} (Fig. 4B), results in a periodic behavior of small action potentials riding on a depolarized plateau interspersed with silent, hyperpolarized phases. Making small changes to several parameters is also a way to simulate bursting activity: using the parameters for activation of the Kv-current estimated by Herrington et al. (19), assuming a 2-fold slower activation of HERG channels (τ_{mHERG} = 200 ms, (26)), lowering the K(ATP)-conductance 3-fold to $g_{K(ATP)} = 0.005$ nS/pF, and shifting the sodium and potassium reversal potentials slightly to $V_{Na} = 90$ mV and $V_K = -70$ mV, respectively, results in a pattern resembling fast square-wave bursting (Fig. 4C). In the model, the HERG current is responsible for shifting between the active and silent phases, as illustrated by the sawtooth-like behavior of the activation variable x_{HERG} (Fig. 4, dashed, blue curves).

The capability of the delayed rectifier to change spiking behavior to bursting electrical activity is experimentally testable. Braun et al. (3) reported that the Kv2.1/Kv2.2 antagonist stromatoxin-1 inhibited the current believed to be carried by the delayed rectifier by ∼40-50 % but had only a weak effect on electrical activity with a tendency to increase the spike height (3) and to broaden the action potentials (M. Braun, University of Oxford, UK, personal communications, 2010). Reducing the delayed rectifier conductance g_{Kv} by 50 % in the model with default parameters reproduces these results. The spiking activity is slightly faster, action potentials peak slightly higher,

and action potentials are broadened (Fig. 5A). Apparently, application of stromatoxin-1 is insufficient in reducing Kv-currents and inducing bursting electrical activity. To enter the bursting regime in the model with default parameters, g_{Kv} needs to be reduced by >70 %.

The broad-spectrum potassium channel blocker tetraethylammonium (TEA) is more potent than stromatoxin-1, and 10 mM TEA reduces Kv-currents by $\sim$ 75-80% in human β-cells (3, 19), and blocks BK-channels completely (3). Model simulations show that reducing g_{Kv} to 0.25 nS/pA while setting $g_{BK} = 0$ nS/pA results in relaxation oscillator-like, "plateau" bursting electrical activity with a nearly flat active phase (Fig. 5B). Adding a modest degree of noise to the right-hand side of Eq. 1 induces spikes in the active phase (Fig. 5C). Noise is inevitably present in biological recordings due to stochastic fluctuations of e.g. ion channels, and has previously been included in β-cell models (29, 39, 41). Spikes can also be induced by modifying the time-constant of L-type Ca^{2+}-channel inactivation ($\tau_{hCaL} = 6$ ms) (not shown). The model prediction of TEA-induced bursting has been observed experimentally, since TEA application often yields bursting behavior (M. Braun, University of Oxford, UK, personal communications, 2010). Assuming a 50 % higher HERG-channel conductance in addition to the TEA-induced reductions in Kv- and BK-conductances ($g_{HERG} = 0.3$ nS/pF, $g_{Kv} = 0.25$ nS/pF, $g_{BK} = 0$ nS/pF) yields the "classical" pattern in β-cells exposed to TEA (3, 33, 34) of large, broad action potentials (Fig. 5B). Finally, blocking BK-channels selectively yields spiking activity with significantly higher action potentials in experiments using iberiotoxin (3) as well as in model simulations ($g_{BK} = 0$ nS/pA; Fig. 5A), suggesting an important role for BK-channels in repolarization after an action potential.

Discussion

The present work described the development of a model including the voltage-gated potassium, sodium and calcium currents present in human β-cells. Model parameters were taken directly from published data whenever possible to reduce parameter tweaking to a minimum. The model satisfactorily reproduced glucose-induced spiking electrical activity (Fig. 2) as well as a series of published data of pharmacologically perturbed situations (Figures 2C, 3, 5). As for mathematical models of rodent β-cells, a central role of K(ATP)-channels was established, since the spike frequency is inversely proportional to the conductance $g_{K(ATP)}$ (Fig. 2A).

It has been suggested (35) that pharmacological modulation of a leak

current, such as the Na^+ leak channel, non-selective (NALCN), could be a target for diabetes treatment. The model supports this idea. The predicted increase in spike frequency, at fixed $g_{K(ATP)}$ value, induced by a raised leak conductance (Fig. 2B), would plausibly result in augmented insulin secretion at a given glucose concentration. In addition, the value for $g_{K(ATP)}$ below which the model produces action potentials can be shifted by modulating the leak current. For example, raising the leak conductance two-fold to $g_{leak} = 0.030$ nS/pF increases the $g_{K(ATP)}$ threshold value to ~ 0.028 nS/pF. This shift in $g_{K(ATP)}$ threshold value suggests that the β-cell would be active at lower glucose concentrations, but importantly and in contrast to treatment with K(ATP)-channel blockers such as sulphonylureas, the β-cell would shut down when the plasma glucose concentration falls to sufficiently, possibly dangerously, low levels.

Similarly, blocking the HERG current increases the spike frequency both in model simulations (Fig. 2D) and experiments (18). Blockage of HERG channels also shifts the $g_{K(ATP)}$ threshold value for electrical activity to $\sim$0.031 nS/pF in the model. Thus, HERG channel blockers could show the same positive characteristics as leak current activators discussed above: increased electrical activity at a given glucose concentration, and a left shift, with respect to glucose, of the activity threshold. Indeed, HERG channel antagonists have been found to enhance insulin secretion (18, 25).

With reasonable parameter changes the model was capable of producing fast bursting activity (Fig. 4). Since bursting is most often observed in clusters of β-cells, one might speculate that small differences in current properties between single β-cells and cells located in clusters underlie the patterns. In mice, such differences have been found between isolated β-cells and cells located in islets (36). Another important difference is that human β-cells are coupled by gap junctions when located in clusters or islets (37). Mathematical modeling has shown that gap junction coupling can turn spiking cells into bursters, especially with help from heterogeneity and noise (38–41). Preliminary simulations of two coupled model cells, using the present model of human β-cells, did not find such a beneficial effect of gap junction coupling (M.G.P., unpublished). A more detailed modeling investigation of coupled human β-cells is left for future studies.

The model did not include Ca^{2+}-regulated SK potassium channels, which have recently been shown to exist in human β-cells (42), and likely play an important role in rodent β-cells (42, 43). This omission was a choice based on the near-total absence of knowledge of the regulation of these channels in human β-cells. Moreover, including the SK-channels would require a model of Ca^{2+} dynamics with even more unknown kinetic constants for Ca^{2+} pumps,

buffering and internal stores. Since the main scope of the present model was to investigate whether the published characteristics of voltage-gated ion channels were sufficient to explain the observed electrical patterns, while minimizing the level of freedom for the choice of model parameters, modeling of SK-channels was left for future work. A careful characterization of SK-channels, of the relation between glucose concentration and K(ATP)-channel conductance, of L-type Ca^{2+}-channel inactivation, and of inactivation properties and V- and Ca^{2+}-regulation of BK-channels, will be essential for further developments of the presented model.

Several studies have found slow Ca^{2+} oscillations (17, 44, 45) and pulsatile insulin secretion (46, 47) with a period of several minutes in human islets. It is tempting to speculate that these oscillations have a metabolic origin, as has been suggested for rodent islets (9, 48), and that electrical activity, which was studied here, is modulated periodically due to oscillating K(ATP)-channel activity. The present work could serve as the foundation for theoretical studies of the interplay between metabolism, calcium and electrical activity, as has been done for rodent studies (9, 10, 12).

Acknowledgments

The author thanks Matthias Braun, University of Oxford, UK, for stimulating conversations and for sharing unpublished results.

Grants

This work was supported by the Lundbeck Foundation, and by the EU through a Marie Curie Intra-European Fellowship.

References

1. Misler, S., D. W. Barnett, K. D. Gillis, and D. M. Pressel, 1992. Electrophysiology of stimulus-secretion coupling in human beta-cells. *Diabetes* 41:1221–1228.

2. Henquin, J.-C., D. Dufrane, and M. Nenquin, 2006. Nutrient control of insulin secretion in isolated normal human islets. *Diabetes* 55:3470–3477.

3. Braun, M., R. Ramracheya, M. Bengtsson, Q. Zhang, J. Karanauskaite, C. Partridge, P. R. Johnson, and P. Rorsman, 2008. Voltage-gated ion

channels in human pancreatic beta-cells: electrophysiological characterization and role in insulin secretion. *Diabetes* 57:1618–1628.

4. Meissner, H. P., and H. Schmelz, 1974. Membrane potential of beta-cells in pancreatic islets. *Pflügers Arch.* 351:195–206.

5. Dean, P. M., and E. K. Matthews, 1968. Electrical activity in pancreatic islet cells. *Nature* 219:389–390.

6. Rorsman, P., 1997. The pancreatic beta-cell as a fuel sensor: an electrophysiologist's viewpoint. *Diabetologia* 40:487–495.

7. Chay, T. R., and J. Keizer, 1983. Minimal model for membrane oscillations in the pancreatic beta-cell. *Biophys J* 42:181–190.

8. Bertram, R., and A. Sherman, 2005. Negative calcium feedback: the road from Chay-Keizer. *In* Bursting: The Genesis of Rhythm in the Nervous System. S. Coombes, and P. C. Bressloff, editors. World Scientific, Singapore. Chapter 2, 19–48.

9. Bertram, R., L. Satin, M. G. Pedersen, D. Luciani, and A. Sherman, 2007. Interaction of Glycolytic and Mitochondrial Dynamics Drives Diverse Patterns of Calcium Oscillations in Pancreatic β-Cells. *Biophys. J.* 92:1544–1555.

10. Fridlyand, L. E., N. A. Tamarina, and L. H. Philipson, 2010. Bursting and calcium oscillations in pancreatic beta cells: specific pacemakers for specific mechanisms. *Am J Physiol Endocrinol Metab.* In Press. doi:10.1152/ajpendo.00177.2010.

11. Meyer-Hermann, M. E., 2007. The electrophysiology of the beta-cell based on single transmembrane protein characteristics. *Biophys J* 93:2952–2968.

12. Pedersen, M. G., 2009. Contributions of mathematical modeling of Beta cells to the understanding of Beta-cell oscillations and insulin secretion. *J Diabetes Sci Technol* 3:12–20.

13. Falke, L. C., K. D. Gillis, D. M. Pressel, and S. Misler, 1989. 'Perforated patch recording' allows long-term monitoring of metabolite-induced electrical activity and voltage-dependent Ca2+ currents in pancreatic islet B cells. *FEBS Lett* 251:167–172.

14. Pressel, D. M., and S. Misler, 1990. Sodium channels contribute to action potential generation in canine and human pancreatic islet B cells. *J Membr Biol* 116:273–280.

15. Barnett, D. W., D. M. Pressel, and S. Misler, 1995. Voltage-dependent Na+ and Ca2+ currents in human pancreatic islet beta-cells: evidence for roles in the generation of action potentials and insulin secretion. *Pflugers Arch* 431:272–282.

16. Cabrera, O., D. M. Berman, N. S. Kenyon, C. Ricordi, P.-O. Berggren, and A. Caicedo, 2006. The unique cytoarchitecture of human pancreatic islets has implications for islet cell function. *Proc. Natl. Acad. Sci.* 103:2334–2339.

17. Quesada, I., M. G. Todorova, P. Alonso-Magdalena, M. Beltrá, E. M. Carneiro, F. Martin, A. Nadal, and B. Soria, 2006. Glucose induces opposite intracellular Ca2+ concentration oscillatory patterns in identified alpha- and beta-cells within intact human islets of Langerhans. *Diabetes* 55:2463–2469.

18. Rosati, B., P. Marchetti, O. Crociani, M. Lecchi, R. Lupi, A. Arcangeli, M. Olivotto, and E. Wanke, 2000. Glucose- and arginine-induced insulin secretion by human pancreatic beta-cells: the role of HERG K(+) channels in firing and release. *FASEB J* 14:2601–2610.

19. Herrington, J., M. Sanchez, D. Wunderler, L. Yan, R. M. Bugianesi, I. E. Dick, S. A. Clark, R. M. Brochu, B. T. Priest, M. G. Kohler, and O. B. McManus, 2005. Biophysical and pharmacological properties of the voltage-gated potassium current of human pancreatic beta-cells. *J Physiol* 567:159–175.

20. Fridlyand, L. E., D. A. Jacobson, A. Kuznetsov, and L. H. Philipson, 2009. A model of action potentials and fast Ca2+ dynamics in pancreatic beta-cells. *Biophys J* 96:3126–3139.

21. Kelly, R. P., R. Sutton, and F. M. Ashcroft, 1991. Voltage-activated calcium and potassium currents in human pancreatic beta-cells. *J Physiol* 443:175–192.

22. Plant, T. D., 1988. Properties and calcium-dependent inactivation of calcium currents in cultured mouse pancreatic B-cells. *J Physiol* 404:731–747.

23. Sherman, A., J. Keizer, and J. Rinzel, 1990. Domain model for Ca2(+)-inactivation of Ca2+ channels at low channel density. *Biophys J* 58:985–995.

24. Fakler, B., and J. P. Adelman, 2008. Control of K(Ca) channels by calcium nano/microdomains. *Neuron* 59:873–881.

25. Hardy, A. B., J. E. M. Fox, P. R. Giglou, N. Wijesekara, A. Bhattacharjee, S. Sultan, A. V. Gyulkhandanyan, H. Y. Gaisano, P. E. MacDonald, and M. B. Wheeler, 2009. Characterization of Erg K+ channels in alpha- and beta-cells of mouse and human islets. *J Biol Chem* 284:30441–30452.

26. Schönherr, R., B. Rosati, S. Hehl, V. G. Rao, A. Arcangeli, M. Olivotto, S. H. Heinemann, and E. Wanke, 1999. Functional role of the slow activation property of ERG K+ channels. *Eur J Neurosci* 11:753–760.

27. Sanguinetti, M. C., C. Jiang, M. E. Curran, and M. T. Keating, 1995. A mechanistic link between an inherited and an acquired cardiac arrhythmia: HERG encodes the IKr potassium channel. *Cell* 81:299–307.

28. Ermentrout, G., 2002. Simulating, analyzing, and animating dynamical systems: A guide to XPPAUT for researchers and students. SIAM Books, Philadelphia.

29. Pedersen, M. G., 2007. Phantom bursting is highly sensitive to noise and unlikely to account for slow bursting in beta-cells: considerations in favor of metabolically driven oscillations. *J Theor Biol* 248:391–400.

30. Misler, S., D. W. Barnett, D. M. Pressel, K. D. Gillis, D. W. Scharp, and L. C. Falke, 1992. Stimulus-secretion coupling in beta-cells of transplantable human islets of Langerhans. Evidence for a critical role for Ca2+ entry. *Diabetes* 41:662–670.

31. Misler, S., A. Dickey, and D. W. Barnett, 2005. Maintenance of stimulus-secretion coupling and single beta-cell function in cryopreserved-thawed human islets of Langerhans. *Pflugers Arch* 450:395–404.

32. Braun, M., R. Ramracheya, P. R. Johnson, and P. Rorsman, 2009. Exocytotic properties of human pancreatic beta-cells. *Ann N Y Acad Sci* 1152:187–193.

33. Atwater, I., B. Ribalet, and E. Rojas, 1979. Mouse pancreatic beta-cells: tetraethylammonium blockage of the potassium permeability increase induced by depolarization. *J Physiol* 288:561–574.

34. Hoppa, M. B., S. Collins, R. Ramracheya, L. Hodson, S. Amisten, Q. Zhang, P. Johnson, F. M. Ashcroft, and P. Rorsman, 2009. Chronic palmitate exposure inhibits insulin secretion by dissociation of Ca(2+) channels from secretory granules. *Cell Metab* 10:455–465.

35. Gilon, P., and P. Rorsman, 2009. NALCN: a regulated leak channel. *EMBO Rep* 10:963–964.

36. Göpel, S., T. Kanno, S. Barg, J. Galvanovskis, and P. Rorsman, 1999. Voltage-gated and resting membrane currents recorded from B-cells in intact mouse pancreatic islets. *J Physiol* 521 Pt 3:717–728.

37. Serre-Beinier, V., D. Bosco, L. Zulianello, A. Charollais, D. Caille, E. Charpantier, B. R. Gauthier, G. R. Diaferia, B. N. Giepmans, R. Lupi, P. Marchetti, S. Deng, L. Buhler, T. Berney, V. Cirulli, and P. Meda, 2009. Cx36 makes channels coupling human pancreatic beta-cells, and correlates with insulin expression. *Hum Mol Genet* 18:428–439.

38. Smolen, P., J. Rinzel, and A. Sherman, 1993. Why pancreatic islets burst but single β cells do not. The heterogeneity hypothesis. *Biophys. J.* 64:1668–80.

39. de Vries, G., and A. Sherman, 2000. Channel sharing in pancreatic beta -cells revisited: enhancement of emergent bursting by noise. *J Theor Biol* 207:513–530.

40. de Vries, G., and A. Sherman, 2001. From spikers to bursters via coupling: help from heterogeneity. *Bull Math Biol* 63:371–391.

41. Pedersen, M. G., 2005. A comment on noise enhanced bursting in pancreatic beta-cells. *J. Theor. Biol.* 235:1–3.

42. Jacobson, D. A., F. Mendez, M. Thompson, J. Torres, O. Cochet, and L. H. Philipson, 2010. Calcium-activated and voltage-gated potassium channels of the pancreatic islet impart distinct and complementary roles during secretagogue induced electrical responses. *J Physiol.* In Press. doi:10.1113/jphysiol.2010.190207.

43. Zhang, M., K. Houamed, S. Kupershmidt, D. Roden, and L. S. Satin, 2005. Pharmacological properties and functional role of Kslow current in mouse pancreatic beta-cells: SK channels contribute to Kslow tail current and modulate insulin secretion. *J Gen Physiol* 126:353–363.

44. Kindmark, H., M. Köhler, T. Nilsson, P. Arkhammar, K. L. Wiechel, P. Rorsman, S. Efendic, and P. O. Berggren, 1991. Measurements of cytoplasmic free Ca^{2+} concentration in human pancreatic islets and insulinoma cells. *FEBS Lett.* 291:310–314.

45. Martin, F., and B. Soria, 1996. Glucose-induced $[Ca^{2+}]_i$ oscillations in single human pancreatic islets. *Cell Calcium* 20:409–414.

46. Marchetti, P., D. W. Scharp, M. Mclear, R. Gingerich, E. Finke, B. Olack, C. Swanson, R. Giannarelli, R. Navalesi, and P. E. Lacy, 1994. Pulsatile insulin secretion from isolated human pancreatic islets. *Diabetes* 43:827–830.

47. Ritzel, R. A., J. D. Veldhuis, and P. C. Butler, 2003. Glucose stimulates pulsatile insulin secretion from human pancreatic islets by increasing secretory burst mass: dose-response relationships. *J Clin Endocrinol Metab* 88:742–747.

48. Tornheim, K., 1997. Are metabolic oscillations responsible for normal oscillatory insulin secretion. *Diabetes* 46:1375–1380.

Table

Parameter			Ref.	Parameter			Ref.
V_K	-75	mV	(3)	V_{Na}	70	mV	$*$
V_{Ca}	65	mV	$*$	$g_{K(ATP)}$	0.015	nS/pF	(1)
g_{leak}	0.015	nS/pF	(1)	V_{leak}	-30	mV	+
g_{CaT}	0.050	nS/pF	(3)	τ_{hCaT}	7	ms	(3)
V_{mCaT}	-40	mV	(3)	n_{mCaT}	-4	mV	(3)
V_{hCaT}	-64	mV	(3)	n_{hCaT}	8	mV	(3)
g_{CaPQ}	0.170	nS/pF	(3)				
V_{mCaPQ}	-10	mV	(3)	n_{mCaPQ}	-10	mV	(3)
g_{CaL}	0.140	nS/pF	(3)	τ_{hCaL}	20	ms	$*$
V_{mCaL}	-25	mV	(3)	n_{mCaL}	-6	mV	(3)
V_{hCaL}	-42	mV	+ (21)	n_{hCaL}	6	mV	+ (21)
g_{Na}	0.400	nS/pF	(3)	τ_{hNa}	2	ms	(3)
V_{mNa}	-18	mV	(3)	n_{mNa}	-5	mV	(3)
V_{hNa}	-42	mV	(3)	n_{hNa}	6	mV	(3)
g_{Kv}	1.000	nS/pF	(3)	$\tau_{mKv,0}$	2	ms	(3)
V_{mKv}	0	mV	(3)	n_{mKv}	-10	mV	(3)
$\bar{g}_{BK}$	0.020	nS/pA	(3)	τ_{mBK}	2	ms	(3)
V_{mBK}	0	mV	(3)	n_{mBK}	-10	mV	(3)
B_{BK}	20	pA/pF	(3)	τ_{mHERG}	100	ms	(26)
g_{HERG}	0.200	nS/pF	+ (18)	τ_{hHERG}	50	ms	(18)
V_{mHERG}	-30	mV	(18)	n_{mCaL}	-10	mV	(18)
V_{hCaL}	-42	mV	(18)	n_{hCaL}	17.5	mV	(18)

Table 1: Default parameters used unless mentioned otherwise. ($*$ M. Braun, University of Oxford, UK, personal communications, 2010; + Adjusted.)

Figure Captions

Figure 1

A) Inactivation function of L-type Ca^{2+}-channels with parameters as in Table 1. Assuming a reversal potential of $V_{Ca} = 50$ mV (21) allowed decent fitting to the inactivation of Ca^{2+}-currents measured by Kelly et al. (21) (full, black) when taking into consideration that L-type currents contribute to ∼50 % of the total Ca^{2+}-current in human β-cells (3) as explained in the main text. However, all simulations of electrical activity were done with $V_{Ca} = 65$ mV, which yields stronger inactivation (dotted, blue). B) The time-dependent activation time constant of Kv-channels τ_{mKv} is described by Eq. 8 to reproduce the results of Braun et al. (3).

Figure 2

Model simulations of spiking electrical activity. The simulation with default parameters given in Table 1 is shown by the full, black curve in all panels. A) The K(ATP) conductance is varied from the default $g_{K(ATP)} = 0.015$ nS/pF to $g_{K(ATP)} = 0.008$ nS/pF (dotted, blue) and $g_{K(ATP)} = 0.018$ nS/pF (dashed, red). B) The leak conductance is varied from the default $g_{leak} = 0.015$ nS/pF to $g_{leak} = 0.030$ nS/pF (dotted, blue) and $g_{leak} = 0.010$ nS/pF (dashed, red). C) The leak reversal potential is varied from the default $V_{leak} = -30$ mV to $V_{leak} = -20$ mV (dotted, blue) and $V_{leak} = -35$ mV (dashed, red). D) Block of HERG channels is simulated by changing HERG-conductance from the default $g_{HERG} = 0.2$ nS/pF to $g_{HERG} = 0$ nS/pF (dotted, blue). Increasing the time-constant for HERG activation 5-fold to $\tau_{mHERG} = 500$ ms lowers the spike frequency (dashed, red). Color figures are available in the online version of the article.

Figure 3

Model simulations of the effect of sodium and T- and L-type calcium channel antagonists on spiking electrical activity. A) The effect of TTX is simulated by setting $g_{Na} = 0$ nS/pF (dotted, blue). The simulation with default parameters given in Table 1 is shown by the full, black curve. Aa) A zoom on action potentials from panel A. The spikes have been aligned to help comparison. Ab) A zoom on the action potential peaks in panel Aa shows that blocking the sodium channels lowers the spike height by ∼ 5 mV.

B) As in panel A, but with $g_{K(ATP)} = 0.008$ nS/pF. The effect of TTX is simulated by setting $g_{Na} = 0$ nS/pF (dotted, blue), while the control case use the default $g_{Na} = 0.4$ nS/pF (full, black). C) Block of T-type, respectively L-type, calcium channels is simulated by setting $g_{CaT} = 0$ nS/pF (dotted, blue), respectively $g_{CaL} = 0$ nS/pF (dashed, red). The simulation with default parameters given in Table 1 is shown by the full, black curve. Color figures are available in the online version of the article.

Figure 4

Model simulations of bursting electrical activity. The membrane potential V (full, black curves; left axes) and the activation variable x_{HERG} for the HERG-current (dashed, blue curves; right axes) are shown. A) The activation function $m_{Kv,\infty}$ for the Kv-current was right-shifted by setting $V_{mK} = 18$ mV. B) The total Kv-channel conductance was reduced by setting $g_{Kv} = 0.2$ nS/pF. C) The parameters for activation of the delayed rectifying potassium current were set following Herrington et al. (19): $\tau_{mKv,0} = 10$ ms, $V_{mK} = 5.3$ mV, $n_{mK} = -8.9$ mV. The activation time-constant of HERG channels was raised to $\tau_{mHERG} = 200$ ms, the K(ATP)-conductance was set to $g_{K(ATP)} = 0.005$ nS/pF, and the Na^+ and K^+ reversal potentials were raised slightly to $V_{Na} = 90$ mV and $V_K = -70$ mV, respectively. Color figures are available in the online version of the article.

Figure 5

Model simulations of the effect of potassium channel blockers on electrical activity. A) The effect of stromatoxin-1 was simulated by setting $g_{Kv} = 0.5$ nS/pF (dashed, red), while the effect of iberiotoxin was simulated by setting $g_{BK} = 0$ nS/pF (dotted, blue) The simulation with default parameters given in Table 1 is shown by the full, black curve. B) The effect of TEA was simulated by setting $g_{Kv} = 0.25$ nS/pF and $g_{BK} = 0$ nS/pF resulting in plateau bursting with default $g_{HERG} = 0.2$ nS/pF (full, black), or in broad action potentials assuming $g_{HERG} = 0.3$ nS/pF (dashed, red). C) Adding a modest amount of noise [$0.7\,\Gamma_t$ where Γ_t is a standard Gaussian white-noise process with zero mean and mean square $\langle \Gamma_t, \Gamma_s \rangle = \delta(t-s)$, see also (39, 41)] to Eq. 1 describing the dynamics of the membrane potential V, introduces spikes in the active phase of TEA-induced plateau bursting (full, black curve in panel B).

Figures

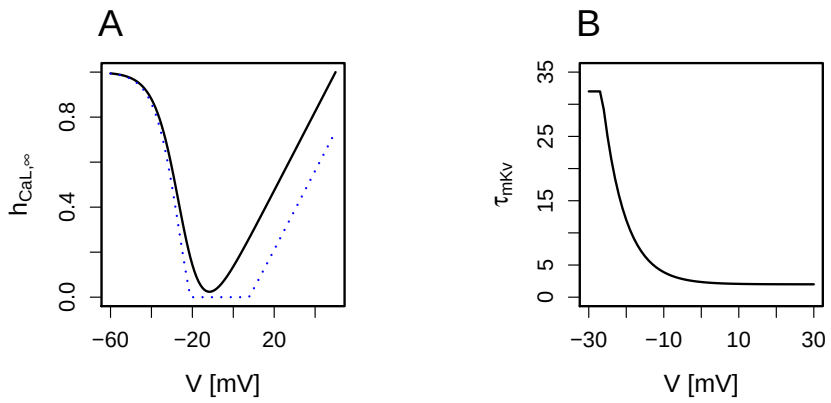

Figure 1:

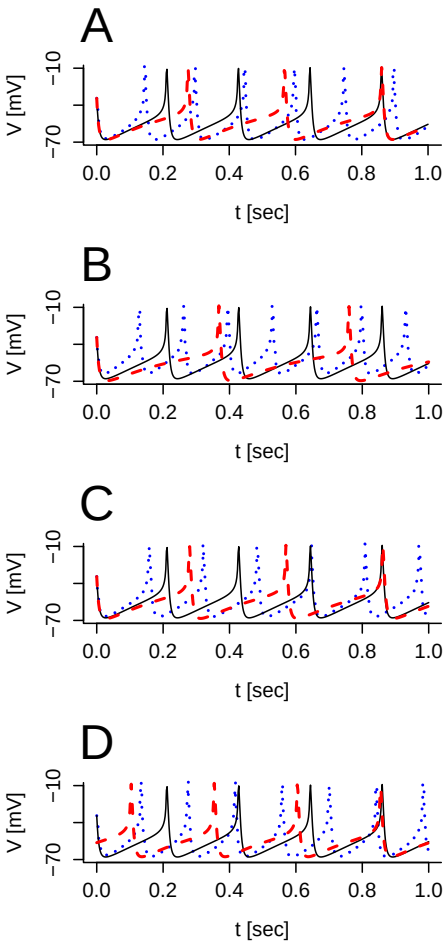

Figure 2:

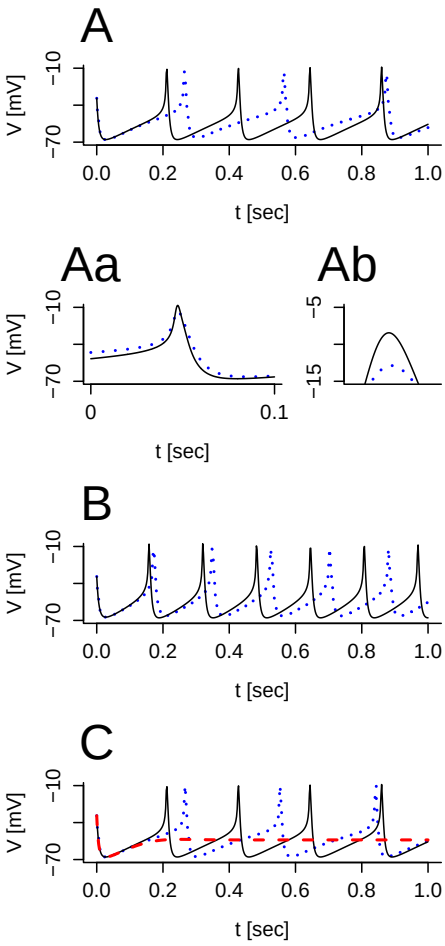
A
V [mV]
−10
−70
0.0
0.2
0.4
0.6
0.8
1.0
t [sec]
Aa
Ab
V [mV]
−10
−70
0
0.1
−5
−15
t [sec]
B
V [mV]
−10
−70
0.0
0.2
0.4
0.6
0.8
1.0
t [sec]
C
V [mV]
−10
−70
0.0
0.2
0.4
0.6
0.8
1.0
t [sec]

Figure 3:

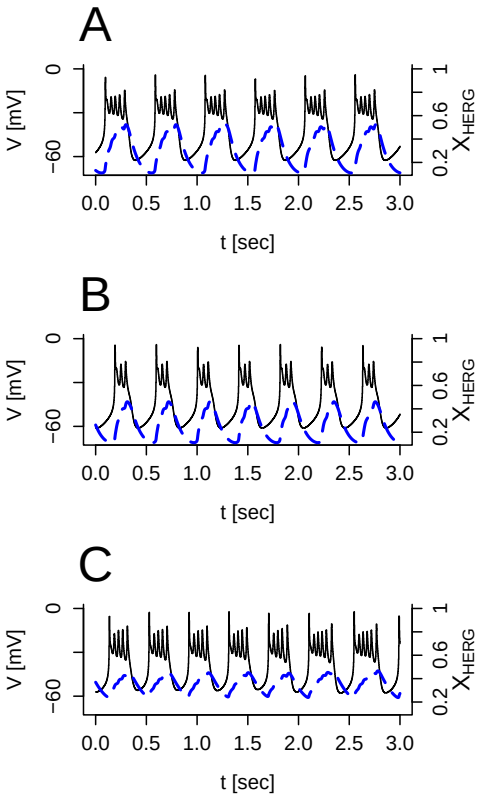
A
V [mV]
0
−60
0.2 0.6 1
X_{HERG}
0.0 0.5 1.0 1.5 2.0 2.5 3.0
t [sec]
B
V [mV]
0
−60
0.2 0.6 1
X_{HERG}
0.0 0.5 1.0 1.5 2.0 2.5 3.0
t [sec]
C
V [mV]
0
−60
0.2 0.6 1
X_{HERG}
0.0 0.5 1.0 1.5 2.0 2.5 3.0
t [sec]

Figure 4:

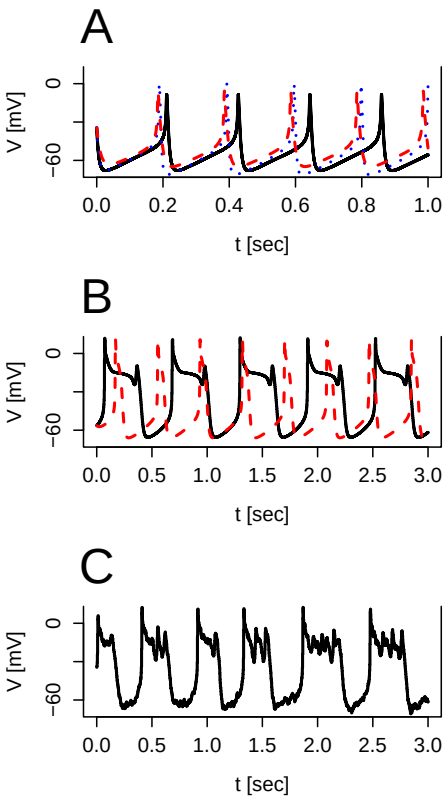
A
V [mV]
0
−60
0.0
0.2
0.4
0.6
0.8
1.0
t [sec]
B
V [mV]
0
−60
0.0
0.5
1.0
1.5
2.0
2.5
3.0
t [sec]
C
V [mV]
0
−60
0.0
0.5
1.0
1.5
2.0
2.5
3.0
t [sec]

Figure 5: